Structural Analysis of Aberrant Chromosomes That Occur Spontaneously in Diploid *Saccharomyces cerevisiae*: Retrotransposon Ty1 Plays a Crucial Role in Chromosomal Rearrangements

Keiko Umezu,*,†,1,2 Mina Hiraoka,*,2,3 Masaaki Mori*,4 and Hisaji Maki*

*Department of Molecular Biology, Graduate School of Biological Sciences, Nara Institute of Science and Technology, Ikoma, Nara 630-0101 and †PREST, Japan Science and Technology Corporation, Kawaguchi, Saitama 332-0012, Japan

ABSTRACT

The structural analysis of aberrant chromosomes is important for our understanding of the molecular mechanisms underlying chromosomal rearrangements. We have identified a number of diploid *Saccharomyces cerevisiae* clones that have undergone loss of heterozygosity (LOH) leading to functional inactivation of the hemizygous *URA3* marker placed on the right arm of chromosome *III*. Aberrant-sized chromosomes derived from chromosome *III* were detected in ∼8% of LOH clones. Here, we have analyzed the structure of the aberrant chromosomes in 45 LOH clones with a PCR-based method that determines the ploidy of a series of loci on chromosome *III*. The alterations included various deletions and amplifications. Sequencing of the junctions revealed that all the breakpoints had been made within repeat sequences in the yeast genome, namely, *MAT-HMR*, which resulted in intrachromosomal deletion, and retrotransposon Ty1 elements, which were involved in various translocations. Although the translocations involved different breakpoints on different chromosomes, all breakpoints were exclusively within Ty1 elements. Some of the resulting Ty1 elements left at the breakpoints had a complex construction that indicated the involvement of other Ty1 elements not present at the parental breakpoints. These indicate that Ty1 elements are crucially involved in the generation of chromosomal rearrangements in diploid yeast cells.

CHROMOSOMAL rearrangements, such as gene amplifications, large deletions, and translocations, are often found in cancer cells and are thus considered to be critical events in the multistep progression to malignancy. It is now widely accepted that one way chromosomal rearrangement can be carcinogenic is that loss of heterozygosity (LOH) results (Lasko *et al.* 1991; Knudson 1993). That is, in the case of a heterozygous cell that contains an inactivating mutation in an allele coding for a tumor-suppressor gene, chromosomal rearrangement could disable the remaining functional allele and thus initiate carcinogenesis. Despite the importance of chromosomal rearrangements in carcinogenesis, however, the molecular mechanisms underlying this process are not well understood. To a certain extent this is due to difficulties in identifying and examining the spontaneous rearrangements that occur in normal cells. It is important to assess the LOH process that occurs in completely normal cells because the mul-

tiple chromosomal rearrangements present in advanced tumors are likely to have arisen, at least in the early stages of the carcinogenesis, from the chromosomal instability that is an intrinsic cellular characteristic of normal cells. Although previous attempts to study spontaneous LOH have found aberrant chromosomes in human T cells and mouse primary fibroblast cells (Gupta *et al.* 1997; Tischfield 1997), the breakpoints of the chromosomal rearrangements were difficult to determine. One reason for this is that mammalian chromosomes are so large that it is not easy to identify the regions involved in chromosomal alterations. Thus, the structural factors that mediate chromosomal aberrations are not well defined in mammalian cells.

The yeast *Saccharomyces cerevisiae* is a good model organism to study chromosomal rearrangements because, compared to mammalian cells, its genome structure is relatively simple and there are a number of technical advantages in the genetic analyses. In haploid yeast cells, detectable levels of spontaneous intrachromosomal deletions can be observed. These deletions occur between repetitive sequences in the yeast genome, including the Ty retrotransposable elements, the ribosomal DNA array, multiple repeats of *CUP1*, and artificially inserted duplicates (Rothstein 1979; Roeder and Fink 1980; Liebman *et al.* 1981; Downs *et al.* 1985; Rothstein *et al.* 1987; Christman *et al.* 1988; Kupiec and Petes 1988; Keil and McWilliams 1993; Klein 1995). Transloca-

---

[1] *Corresponding author:* Department of Molecular Biology, Graduate School of Biological Sciences, Nara Institute of Science and Technology, Takayama 8916-5, Ikoma, Nara 630-0101, Japan. E-mail: umezu@bs.aist-nara.ac.jp

[2] These authors contributed equally to this work.

[3] *Present address:* Genome Science Center, Riken, Yokohama, Kanagawa 230-0045, Japan.

[4] *Present address:* BioResearch Lab., Toyota Motor Co., Toyota, Aichi 471-8572, Japan.

tions and inversions between Ty elements were also observed (Breilmann *et al.* 1985; Rothstein *et al.* 1987; Kupiec and Petes 1988; Rachidi *et al.* 1999). However, a recent analysis of gross chromosomal rearrangements in haploid cells revealed the occurrence, albeit at lower frequencies, of different types of rearrangements that do not require long homologous sequences at breakpoints (Chen *et al.* 1998; Chen and Kolodner 1999; Myung *et al.* 2001a,b). Microhomology- and nonhomology-mediated translocations as well as chromosomal deletions accompanied with telomere additions were observed in both wild-type cells and various mutant cells. Despite these yeast cell analyses, however, it is still difficult to gain an accurate view of spontaneous chromosomal rearrangements in normal cells because the studies mentioned above were all performed with either haploid cells or cells in meiosis, mainly for technical reasons. Mitotic recombination between allelic loci occurs much more frequently than chromosomal rearrangement in diploid yeast cells, which makes it difficult to detect aberrant chromosomes by genetic procedures (Hiraoka *et al.* 2000). The detection of rearrangements is thus technically easier when using haploid rather than diploid cells. However, when haploid cells are used, only a limited portion of the rearrangements can be detected because those chromosomal rearrangements that lead to the loss of an essential gene or DNA segment would make the cells inviable. Consequently, the chromosomal rearrangements that can be detected may be biased toward a particular type. Studying haploid cells thus limits our understanding of the chromosomal structural features that are involved in chromosomal rearrangement, such as particular chromosomal elements or nucleotide sequences. Studying the aberrant chromosomes that are found within a natural diploid genome will provide a more complete picture.

In a previous study, we analyzed the spontaneous LOH events in *S. cerevisiae* diploid cells under vegetative conditions that lead to functional inactivation of the hemizygous *URA3* marker placed at the center of the right arm of chromosome *III* (Hiraoka *et al.* 2000). The frequency of LOH events, which was determined by selection for 5-fluoroorotic acid-resistant progeny, was $1–2 \times 10^{-4}$ by this assay. Analysis of chromosome structure in a large number of LOH clones by pulsed-field gel electrophoresis (PFGE) and PCR showed that the major classes of the events were chromosome loss, allelic recombination, and chromosome size aberration. Chromosome loss contributed to ~60% of all the LOH events, while allelic recombination was responsible for 30–35%. In particular, aberrant-sized chromosomes derived from chromosome *III* were detected readily in ~8% of the LOH clones. This analysis, coupled with a conventional genetic method, allowed us to classify the chromosomal rearrangements into two classes: one caused by intrachromosomal deletion and the other by interchromosomal rearrangement. In the study reported here, we

have further analyzed the structure of the aberrant chromosomes that we isolated. To do this, we developed a PCR-based method that determines the ploidy of a series of loci on chromosome *III*. This method allowed us to identify the regions that were altered in the aberrant chromosomes, either by deletion or amplification, in 45 LOH clones. The junctions of the rearrangements were then amplified by PCR and sequenced to reveal the breakpoints. Analysis of the breakpoints indicated that in diploid yeast cells Ty1 elements play crucial roles in chromosomal rearrangement that are more specific than just providing repetitive sequences for homologous recombination.

MATERIALS AND METHODS

***S. cerevisiae* strains:** Strains YMH1 (*MAT*a *lys2Δ202 leu2Δ1 ura3-52 trp1Δ 63 III*-205::*URA3*) and FY838 (*MAT*α *lys2Δ202 leu2Δ1 ura3-52 his3Δ200*) have been previously described (Hiraoka *et al.* 2000). The strains are derivatives of the S288c heterothallic strain. *III*-205::*URA3* signifies that the *URA3* fragment was inserted at the 205-kb locus of chromosome *III*. Nucleotide coordinates are as given in the Saccharomyces Genome Database (SGD; http://genome-www.stanford.edu/Saccharomyces). Other loci are referred to in a similar manner as *III*-205. That is, the number of the chromosome where the locus is located is hyphenated with the number that represents the position of the locus in a kilobase scale. Strain RD101, which is a parental diploid strain carrying the hemizygous *URA3* marker at the *III*-205 locus, was constructed by crossing YMH1 and FY838. The LOH clones analyzed in this study were all isolated from RD101 and were shown in our previous study (Hiraoka *et al.* 2000) to have an aberrant-sized chromosome derived from chromosome *III* by PFGE (Figure 1). All of the isolates, apart from six that could not be recovered after storage, were analyzed in this study (a total of 45 clones).

Genetic and nucleic acid techniques: Standard genetic manipulations of yeast were performed as previously described (Rose *et al.* 1990; Ausubel *et al.* 1994). Yeast genomic DNA was prepared with the Nucleon yeast mini prep kit (Amersham, Buckinghamshire, England) or the GenTLE yeast kit (Takara, Tokyo). PCR products used as probes in Southern hybridization were purified with the QIAquick PCR purification kit (QIAGEN, Hilden, Germany). General DNA manipulations were performed as previously described (Sambrook *et al.* 1989; Ausubel *et al.* 1994). Restriction fragment length polymorphism (RFLP) of aberrant chromosomes was analyzed by digesting chromosome DNA in an agarose plug (100–200 ng of DNA) with 10 units of the indicated enzyme in 100 μl of the buffer overnight at the appropriate temperature.

PCR procedures: PCR was performed at standard conditions as previously described (Hiraoka *et al.* 2000). Griner Japan (Tokyo) supplied all primers used in this study. To amplify the fragments for DNA sequencing, *Ex Taq* or *Z-Taq* DNA polymerase (Takara) was used. PCR with *Z-Taq* DNA polymerase was carried out as recommended by the manufacturer with a program of an initial incubation at 95° for 1 min followed by 30 cycles of 98° for 1 sec, 58° for 10 sec, and 72° for 1–2 min. Conditions used for quantitative PCR are described below.

PCR-based method to determine the ploidy of multiple loci on chromosome *III*: Specific primer sets were designed for each of 22 loci on chromosome *III* and 2 loci on chromosome *VI* on the basis of the *S. cerevisiae* genome sequence in the SGD database (Figure 2). Nucleotide sequences of the primers

are available upon request. For each primer set, the PCR products were sampled by gel electrophoresis and ethidium bromide staining of the gel to confirm that only products of the expected size were present. One primer of each set was labeled with either 6-FAM or HEX at the 5′ end. Of the 24 primer sets, 17, including 1 set on chromosome *VI*, were labeled with 6-FAM and the remaining 7, including the set for the other locus on chromosome *VI*, were labeled with HEX. The two loci on chromosome *VI* served as a control site, respectively, for 6-FAM or HEX signal to normalize the product amounts of the chromosome *III* loci for each experiment. The product sizes were designed to fall in the range of 139–335 bp in such a way as to differ from other products with the same label by at least 2 bp. For quantitative PCR of the various loci, 3 ng of genomic DNA was used as a template in 25 μl of reaction mixture. Amplification was performed individually for each locus with GeneAmp PCR System 9600 (PE Applied Biosystems, Foster City, CA) with a program consisting of an initial incubation at 95° for 1 min followed by 17 cycles of 92° for 1 min, 60° for 1 min, and 72° for 1 min. After the PCR, 10 μl was withdrawn from the 24 individual reactions. All aliquots were combined into a single tube with 10 μl of distilled water. A portion (∼2 μl) of the mix was combined with 0.5 μl of a ROX-labeled size standard (Genescan-500 ROX, PE Applied Biosystems) and 10 μl of formamide. Samples were denatured at 94° for 4 min and subjected to electrophoresis through POP4 polymers (PE Applied Biosystems) with a capillary sequencer ABI PRISM310 (PE Applied Biosystems). Data were processed with 310 GeneScan software (version 2.1, PE Applied Biosystems) to determine the size and amount of each product. The product amounts for each locus on chromosome *III* were normalized against either of those for the two loci on chromosome *VI* by using Genotyper software (version 2.0, PE Applied Biosystems) in which the signals of 6-FAM and HEX were analyzed separately. The ploidy of the 22 loci in each clone was determined from the ratio of the normalized value relative to the value of the corresponding locus estimated for the parental diploid strain. The analysis was performed at least twice for each clone.

Pulsed-field gel electrophoresis: PFGE analysis of chromosomes was performed with the standard conditions described previously (HIRAOKA *et al.* 2000). For RFLP analysis of chromosomes, the switch time was altered linearly from 0.47 to 10.29 sec for 28 hr 18 min to obtain a higher resolution at the range from 10 to 120 kb.

Southern blotting: Transfer of chromosomal DNA fragments and detection of hybridization were performed as described previously (HIRAOKA *et al.* 2000). Hybridized probes were detected with the Gene Images labeling and detection system (Amersham) according to the protocols of the supplier. Probes were obtained by PCR amplification of the indicated loci. Aberrant chromosomes derived from chromosome *III* were visualized with a pair of probes corresponding to two regions on the left arm of chromosome *III*, *III*-54 and *III*-102, as described previously (HIRAOKA *et al.* 2000). Probes used for the RFLP analysis of the class IV clones corresponded to locus *III*-79 on the left arm and locus *III*-167 on the right arm. For the analysis of translocations in class V clones, which appear to involve sequences from other chromosomes, probes from the following loci were used: *I*-207, *VII*-1054, *X*-587, *XII*-1010, and *XVI*-908.

DNA sequencing: DNA sequencing was carried out by the dye terminator method using BigDye terminator cycle sequencing kits (PE Applied Biosystems) with a capillary sequencer ABI PRISM310 (PE Applied Biosystems). For breakpoint analysis, genomic DNA purified from PFGE plugs was used directly in the reactions. Comparison of DNA sequences was performed with GeneWorks software (version 2.5.1, Oxford Molecular Group, Campbell, CA).
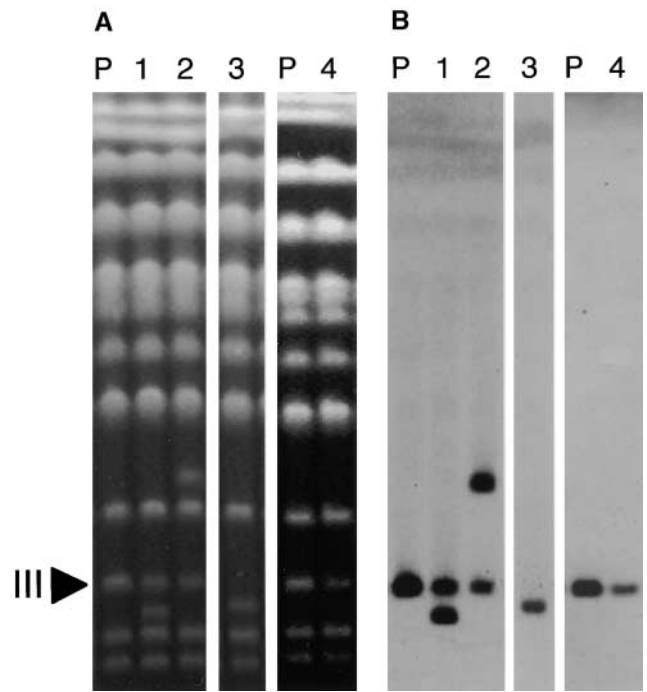

FIGURE 1.—Aberrations of chromosome *III* detected by PFGE and Southern blotting. Chromosome patterns of representative LOH clones (lanes 1–4) and those of parental strain RD101 (marked P) are shown. (A) An ethidium bromide-stained PFGE gel. (B) Southern blotting analysis of the same gel. Probes used corresponded to two regions on the left arm of chromosome *III*, *i.e.*, *III*-54 and *III*-102. A solid triangle indicates the position of the normal chromosome *III*. Lanes 1 and 2, clones that have an aberrant chromosome *III* and its homolog; lane 3, a clone that carries only an aberrant chromosome *III* as its homolog is absent (this clone is classified later into class II-b according to locus ploidy analysis; see Figure 3); lane 4, a clone monosomic for chromosome *III*. All clones shown here were isolated in our previous study (HIRAOKA *et al.* 2000).

RESULTS

PCR-based mapping of the rearranged regions in aberrant chromosomes: We previously analyzed the spontaneous LOH events that lead to functional inactivation of the hemizygous *URA3* marker placed at the center of the right arm of chromosome *III* (*III*-205 locus) in diploid *S. cerevisiae* cells (HIRAOKA *et al.* 2000). The LOH events occurred at a frequency of $1–2 \times 10^{-4}$ and ∼8% of the LOH clones had acquired an aberrant chromosome that was derived from chromosome *III* (Figure 1). The aberrant chromosomes varied in size and were generated by either intrachromosomal deletion or interchromosomal rearrangement. Analysis of the breakpoints of these aberrant chromosomes may assist in elucidating the molecular mechanisms underlying these chromosomal alterations. As the parental strain was constructed by mating two isogenic haploid strains, the aberrant chromosome in the LOH clones was accompanied mostly by its nearly identical homologous chromosome. Thus, to identify the rearranged region of the
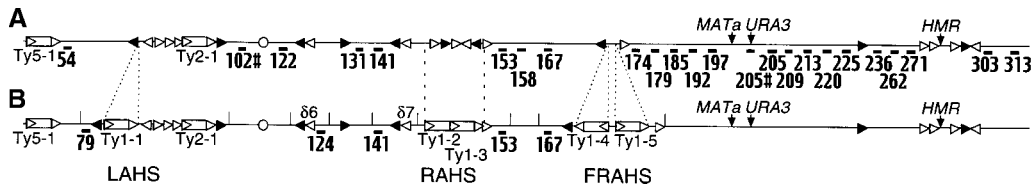
FIGURE 2.—The structure of chromosome *III*. Schematically depicted is the structure of the chromosome *III* according to the SGD database (A) and the chromosome *III* present in the *MAT*a strain YMH1 that was used to construct the parental diploid RD101 strain (B). Chromosome *III* in the *MAT*α strain FY838 has essentially the same structure as that in YMH1 except that it has no *URA3* insert. The horizontal lines represent chromosome *III*. Circles indicate its centromere. Arrows show the *MAT*a and *HMR* loci and the *URA3* insert at *III*-205, as indicated. The dashed lines link the corresponding positions on the two chromosomes. Repetitive sequences such as Ty elements (open rectangles with open triangles at the ends), solo δ sequences (open triangles), and tRNA genes (solid triangles) are marked. The positions of PCR loci used for the ploidy analysis (A) and the probes used in RFLP analysis (B) are indicated as short solid bars at the corresponding chromosome positions. Numbers below the bars represent the locus positions in a kilobase scale according to the SGD database. The two loci marked with a number sign (102# and 205#) indicate those analyzed by quantitative PCR in the previous study (HIRAOKA *et al.* 2000). Vertical lines in B indicate the *Eae*I sites that were used in the RFLP analysis of chromosome *III* in the haploid strains YMH1 and FY838. The scale is not proportional.

aberrant chromosome in the presence of its homolog, we developed a PCR-based method that determines the ploidy of a series of loci on chromosome *III*.

Primer pairs were placed at 22 specific loci over chromosome *III*; 21 were distributed on the right arm at intervals of ∼10 kb, and the remaining locus was on the left arm (Figure 2A). One primer of each pair was labeled with either 6-FAM or HEX so that the PCR product amounts could be quantified from their fluorescence signals. For each experiment, the product amounts were normalized to that of the control loci on chromosome *VI*, separately for each fluorescence signal. PCR was performed individually for each locus in such a way as to be terminated within the phase of exponential amplification and then the products were analyzed simultaneously by a fluorescence-based capillary sequencer. To evaluate whether the PCR-based method can really be used to identify the missing regions on chromosome *III*, a LOH clone monosomic for chromosome *III* (Figure 1, lane 4) was analyzed with the method. For all of the 22 loci on chromosome *III*, the PCR products of the monosomic clone were approximately half as intense as those of the diploid parent strain (Figure 3, chromosome loss). The ratios ranged from 0.39 to 0.60 and the mean was 0.47. This clearly indicates that the PCR method can accurately distinguish haploid from diploid at each locus and so will be useful in identifying the rearranged regions of the aberrant chromosomes derived from chromosome *III*.

The PCR-based ploidy analysis was validated when it was applied to the 45 LOH clones harboring an aberrant chromosome *III* that had been previously isolated and that are the subject of this study. The chromosomal rearrangement breakpoints of 11 of these clones have already been defined previously (HIRAOKA *et al.* 2000). These clones had been found to carry a 94-kb deletion between the *MAT*a and *HMR* loci on chromosome *III*. This caused *MAT*a and *HMR* to fuse faithfully at the breakpoint. The ploidy pattern of these 11 clones, as detected with the PCR-based method (see class I clones in Figure 3), was completely consistent with the previous

observations. That is, the *III*-205 to *III*-271 loci that constitute the deletion were haploid, and the deletion junctions at the *MAT*a and *HMR* loci were within the sites where the ploidy shifted from diploid to haploid, *i.e.*, between *III*-197 and *III*-205 and between *III*-271 and *III*-303, respectively. With the analysis using additional markers on the chromosome, the *MAT*a-*HMR* deletion was shown to occur predominantly as an intrachromosomal deletion and no other kinds of intrachromosonal deletions were detected in LOH clones obtained with wild-type cells (HIRAOKA *et al.* 2000).

Aberrant chromosomes can be classified into five classes on the basis of the ploidy patterns of chromosome *III* loci: The PCR-based method to define locus ploidy was applied to all 45 of the LOH clones that harbor an aberrant chromosome *III* and were previously isolated from the parental diploid strain RD101 that carries the hemizygous *URA3* marker at the *III*-205 locus (HIRAOKA *et al.* 2000). The results are summarized in Figure 3. The clones can be classified into five classes. The 11 clones described above as having a 94-kb deletion between the *MAT*a and *HMR* loci fell into class I. Class II clones can be distinguished from the other classes because the clones bear an aberrant chromosome with the wild-type allele at the *III*-205 locus where the *URA3* marker was originally inserted. Seven class II clones were identified and could be further subdivided according to their ploidy patterns. In class II-a (see Figure 3) clones, the *III*-205 locus was homozygous for the wild-type allele without the insertion. Our previous study showed that class II-b and II-c clones have only an aberrant chromosome without an accompanying homolog (Figure 1, lane 3). The ploidy analysis hence indicated that, like the class II-a clones, the aberrant chromosome *III* in the class II-b and II-c clones carries the wild-type allele at *III*-205. In the other classes, the clones were all hemizygous for the *III*-205 locus and lacked a region that included the *URA3* marker in the aberrant chromosome. In class III and IV clones, a locus on the left arm (*III*-54) had been triplicated and a substantial part of the right arm up to the terminal locus (*III*-313) was
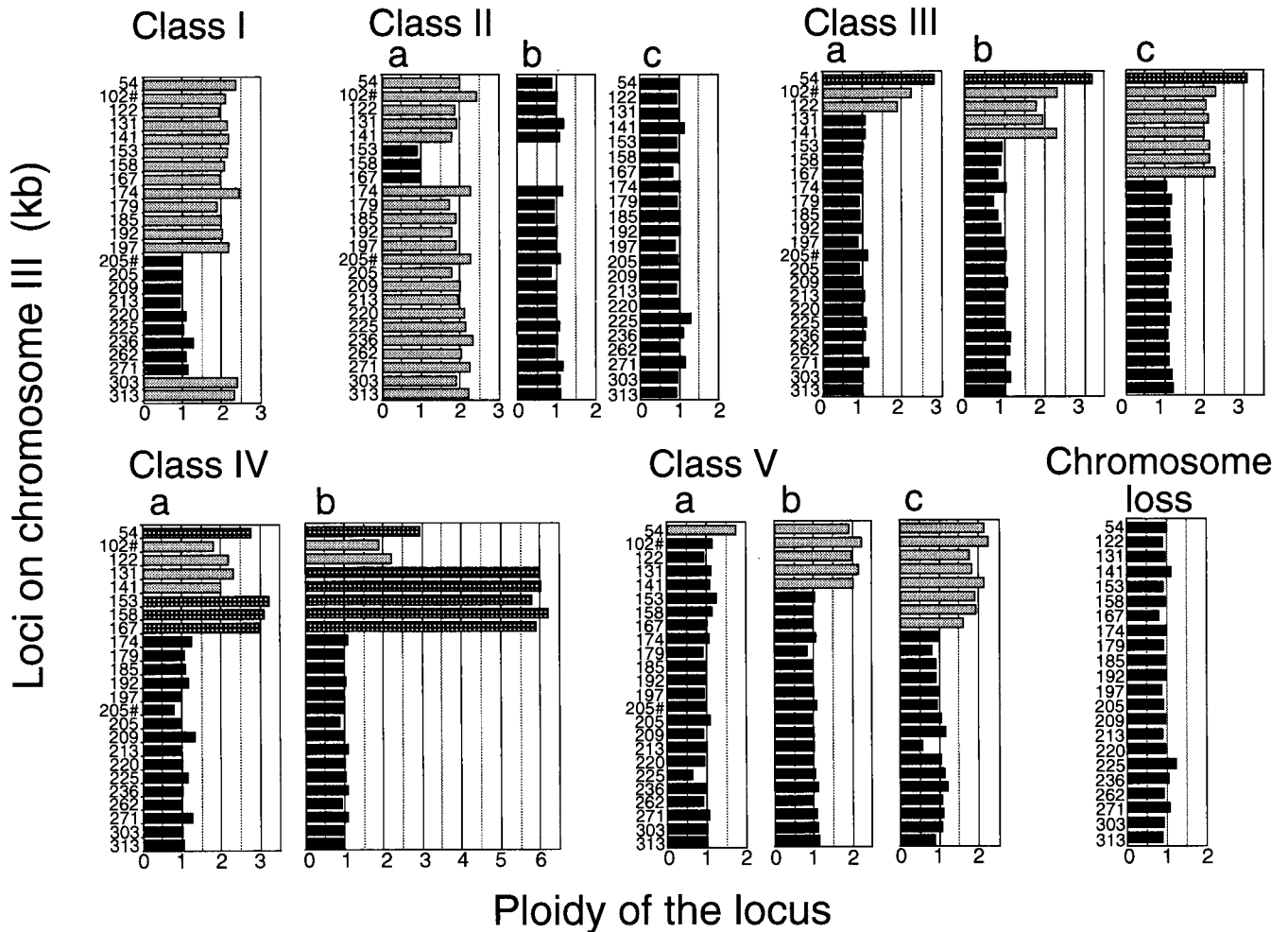
FIGURE 3.—Classification of aberrant chromosomes *III* on the basis of the ploidy of various loci on chromosome *III*. PCR loci are indicated relative to their positions on chromosome *III*. The numbers represent these positions in a kilobase scale according to the SGD database. The two loci marked with a number sign (102# and 205#) indicate those analyzed by quantitative PCR in the previous study (HIRAOKA *et al.* 2000). The ploidy of each locus in the indicated clone was determined by the ratio of the PCR product amount of the locus relative to that of the corresponding locus estimated for the parental diploid strain, as described in MATERIALS AND METHODS. A representative result is shown for each subclass. The result with a clone that is monosomic for chromosome *III* is also shown as a control (marked "chromosome loss"). Solid bars indicate the haploid loci, shaded bars indicate the diploid loci, and dotted bars indicate where loci are more than diploid.

missing. Class IV clones had an additional amplification, up to sixfold in class IV-b, within the right arm. Class V clones had a gross deletion up to the terminal locus on the right arm. The PFGE analysis of the class V clones, however, showed that some of the aberrant chromosomes in these clones were longer than the normal chromosome *III* (Table 1). The discrepancy between these observations suggests that the aberrant chromosome *III* in class V clones may contain a segment derived from other chromosomes by translocations.

Ty1 insertion hotspots on chromosome *III*: In the class II–V clones, the junctions where the ploidy changed were located within the following four regions: between *III*-54 and *III*-102, *III*-122 and *III*-131, *III*-141 and *III*-153, and *III*-167 and *III*-174 (Figure 3). We examined the sequences of these regions in the SGD database and

noticed that all of these regions carry repetitive sequences, including the Ty element, long terminal repeats (LTRs), and tRNA genes. In addition, three of the regions are known to be hotspot sites of Ty insertion and have been called the LAHS (the left arm transposition hotspot), RAHS (the right arm transposition hotspot), and FRAHS (the far right arm transposition hotspot) (Figure 2; WARMINGTON *et al.* 1986, 1987; JI *et al.* 1993; WICKSTEED *et al.* 1994). It is possible that these repetitive sequences may be involved in the rearrangements that generate the aberrant chromosomes. However, the Ty insertion hotspots are known to have variations on Ty insertions even among strains from the same genetic background (OLIVER *et al.* 1992).

The Ty elements in these four regions were located in both of the haploid strains used to construct the pa-

TABLE 1

Aberrant chromosomes in LOH clones isolated from RD101

Size difference (kb) PFGE/map[a]	Class[b]	No. of identified clones (culture)[c]	Elements at the original breakpoints[d]
−80/−94	I	11 (6)	*MAT***a**, *HMR***a**
−40/−35	II-a	2 (2)	Ty1-2, Ty1-5
−30/−29	II-a, b	4 (4)	Ty1-3, Ty1-5
−10/−6	II-c	1 (1)	Ty1-2, Ty1-3
−105/−130	III-a	1 (1)	δ 6, Ty1-1
−105/ND	III-a	1 (1)	ND
−100/−111	III-b	1 (1)	δ 7, Ty1-1
−60/−72	III-c	7 (5)	Ty1-4, Ty1-1
−55/−55	IV-a	3 (2)	Ty1-3, Ty1-1
−50/−50	IV-a	1 (1)	Ty1-3, Ty1-1
−50/−50	IV-a	3 (2)	Ty1-2, Ty1-1
+145/+145	IV-b	1 (1)	Ty1-4, Ty1-1
−110/ND	V-c	1 (1)	ND
−80/ND	V-b	1 (1)	ND
−80/−90	V-c	1 (1)	Ty1-4, (*I*) Ty1-1
−25/−17	V-c	1 (1)	Ty1-4, (*XVI*) Ty1-2
+110/+85	V-b	1 (1)	Ty1-3, (*X*) Ty1-2
+210/ND	V-a	1 (1)	ND
+250/+239	V-b	1 (1)	Ty1-2, (*XII*) Ty1-3
+380/+366	V-b	1 (1)	Ty1-2, (*VII*) Ty1-1
+380/+372	V-b	1 (1)	Ty1-3, (*VII*) Ty1-1

ND, not determined.

[a] The difference in size of the aberrant chromosome relative to the 330-kb wild-type chromosome *III* is indicated. The size of the aberrant chromosome was determined by PFGE of the clone, which is indicated before the slash. After the breakpoints were determined, the expected size of the aberrant chromosome was calculated on the basis of the physical map in the SGD database, which is indicated after the slash.

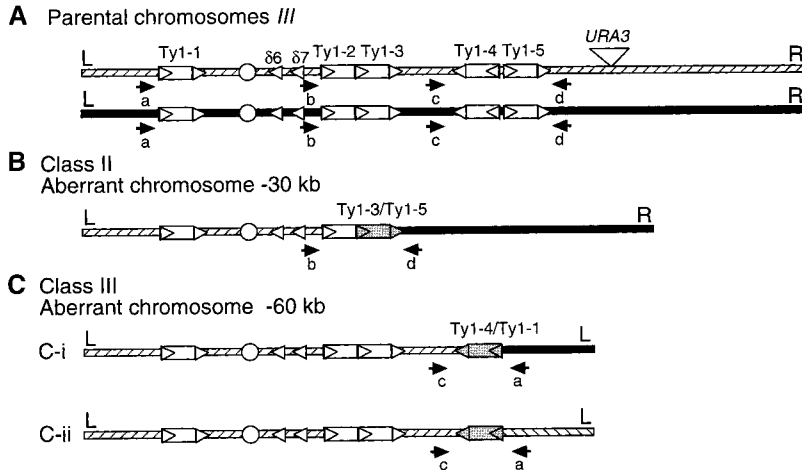[b] Classification by the PCR-based chromosome scanning shown in Figure 3.

[c] The number of clones is shown together with the number of independent cultures from which the clones were isolated (indicated in parentheses). In total, 640 clones from 18 cultures were analyzed.

[d] DNA elements detected at the junctions on the parental chromosomes are indicated. Ty1 and δ elements are designated with the number that denotes their relative position on the chromosome. The designation of Ty1 elements on chromosome *III* is described in the text, while the designation of the other elements is as given in the SGD database. For the elements on chromosomes other than chromosome *III*, the number of the chromosome is indicated in the parentheses in front of the element description.

rental diploid RD101. The results are summarized in Figure 2B. First, the presence of Ty insertions was surveyed by RFLP analysis of the regions. Thus, genomic DNA was digested with *Eae*I that does not cut within Ty sequences and was hybridized with probes that correspond to the junction regions (Figure 2B). The region shown to contain the insertion was then amplified by PCR with primers encompassing the region and the PCR products were sequenced to determine the position and orientation of the insertion. The major structural differences between the chromosome *III* in our strains and that depicted in the SGD database are as follows (Figure 2): In both of our haploid strains, chromosome *III* contained five novel Ty1 elements and one additional LTR of Ty3, also called the σ sequence. The Ty1 elements are designated here as Ty1-1 to Ty1-5 in the order of

their location from the left end of the chromosome. In the region between *III*-141 and *III*-153 that constitutes the RAHS site of Ty insertion, two segments that exist in the SGD database were missing in our strains. One is a 102-bp segment between a 10-bp direct repeat around the *III*-142 locus. The other is a 3-kb segment from *III*-148 to *III*-151. The latter deletion is accompanied by an insertion of tandemly arranged Ty1-2 and Ty1-3, which share an LTR also called the δ sequence (Figure 2B). These observations were used to further analyze the aberrant chromosomes of the class II–V clones.

Unequal crossing over between Ty1 elements on the right arm of chromosome *III* in class II clones: The PCR-based scanning of chromosome *III* allowed us to classify class II clones as those that bear an aberrant chromosome with the wild-type allele at *III*-205 (Figure

A Parental chromosomes *III*

B Class II
Aberrant chromosome -30 kb

C Class III
Aberrant chromosome -60 kb

FIGURE 4.—Aberrant chromosomes in class II and III clones. The structures of representative aberrant chromosomes found in class II (B) and class III (C) clones are presented schematically and compared with the chromosome *III* pair found in the parental strain RD101 (A). Hatched bars depict the chromosome *III* that was inserted with the *URA3* marker (an open triangle) at the *III*-205 locus. Solid bars indicate its homolog and circles show their centromeres. Ty1 elements (rectangles with triangles at the ends) and solo δ sequences (triangles) that are related to the aberrant chromosomes are indicated. The Ty1-element hybrids detected at the breakpoints are shaded. The letters L and R indicate the left end and the right end of chromosome *III*, respectively. Arrows show the primers used to amplify the breakpoints of the aberrant chromosomes (see text for the designation of a–d). B depicts a 30-kb-shorter aberrant chromosome in a class II clone and C shows a 60-kb-shorter aberrant chromosome in a class III clone. In the latter, two kinds of alternative structures of the aberrant chromosome are shown: the one generated by recombination between the homologs (C-i) and another formed within the chromosome (or between the sister chromatids; C-ii).

3). This strongly suggests that the *URA3* insertion has been replaced with its allelic locus *III*-205, presumably through unequal crossing over within the *CEN3-III*-205 interval between homologous chromosomes.

With respect to the three subclasses in class II, the class II-a and II-b clones had essentially identical ploidy patterns because the class II-b clones bear only the aberrant chromosome *III*, unaccompanied by its homolog (Figure 1, lane 3), while the aberrant chromosome *III* in class II-a clones coexists with its normal homolog. Thus, the aberrant chromosomes in class II-a and II-b clones lack the region between *III*-153 and *III*-167 (Figure 3). Consequently, the putative rearrangement junctions exist between *III*-141 and *III*-153 and between *III*-167 and *III*-174, respectively. Both of these regions occur within the *CEN3-III*-205 interval. As shown in Figure 2, the RAHS and FRAHS sites are juxtaposed to the missing regions. Both of these sites contain Ty1 elements in the same orientation, namely, Ty1-2 and Ty1-3 in RAHS, and Ty1-5 in FRAHS, respectively. The interval between Ty1-2 and Ty1-5 is 35 kb while that between Ty1-3 and Ty1-5 is 29 kb. These sizes agree well with the PFGE analysis of the clones, which showed that the aberrant chromosomes are 40 or 30 kb shorter than the original chromosome (Table 1). These results strongly suggest that the aberrant chromosomes have been generated by recombination between the 5.9-kb direct repeat of Ty1, *i.e.*, either between Ty1-2 and Ty1-5 or between Ty1-3 and Ty1-5. This idea was tested by amplifying the putative junctions of the aberrant chromosomes by PCR with primers that encompass Ty1-2 and Ty1-5 from both sides (Figure 4, primers b and d). While the primer sites are located more than 40 kb apart on the normal chromosome *III*, which is too far for efficient amplification, all of the class II-a and II-b clones could nevertheless be successfully amplified. The product size was 12 kb in the four clones with a 30-kb-shorter chromo-

some (Figure 4B) and 6 kb in the two clones with a 40-kb-shorter chromosome. DNA sequencing of the PCR products confirmed that Ty1 element pairs were actually fused at the junction (Table 1). In the 30-kb-shorter chromosomes, Ty1-3 and Ty1-5 had been fused, leaving one Ty1 element at the joint and deleting the region between them (Figure 4B). The 40-kb-shorter chromosomes were fused between Ty1-2 and Ty1-5 by deleting the region between them.

In the only class II-c clone, which was shown to have only one aberrant-sized chromosome *III* without an accompanying homolog, a missing region was not detected on the chromosome by the PCR-based chromosome scanning (Figure 3). PFGE analysis of the clone showed that the aberrant chromosome was only 10 kb shorter than the original (Table 1), and thus it is possible that the region that is missing is not in the sites analyzed by the PCR. All the results obtained with the clone are consistent with the notion that the aberrant chromosome resulted from a fusion between tandemly repeated Ty1-2 and Ty1-3 elements similar to what was observed for the other class II clones. That is, PCR amplification of the region encompassing these two Ty elements yielded 6.5-kb products, while 13-kb products were obtained when the parent strain was tested. DNA sequencing of the class II-c products revealed that Ty1-2 and Ty1-3 had been faithfully fused into one Ty1 element and that the 5.6-kb sequence between them had been deleted. The size of the deletion is consistent with that determined by PFGE, whose limit of resolution around chromosome *III* was ∼5–10 kb (Table 1).

In summary, all of the seven class II aberrant chromosomes were formed by the fusion of tandemly repeated Ty1 elements within the *CEN3-III*-205 interval (Table 1) and are likely to have been generated by recombination between the homologous chromosomes.

Nonreciprocal translocations of the left arm to the

right arm of chromosome *III* in class III clones: In the class III clones, a locus on the left arm (*III*-54) had been triplicated and a substantial part of the right arm up to the terminal locus (*III*-313) was missing (Figure 3). These observations indicate that the aberrant chromosome *III* in class III clones bears a duplication of a region on the left arm and a gross deletion in the right arm. Ten clones were classified into class III and further divided into three subclasses according to the centromeric junction of the missing region in the right arm (Table 1 and Figure 3). The junctions were between *III*-122 and *III*-131 for class III-a, between *III*-141 and *III*-153 for class III-b, and between *III*-167 and *III*-174 for class III-c. Intriguingly, the last two junction regions cited were also those found to be involved in class II. These two regions contain RAHS and FRAHS, respectively (Figure 2).

It is possible that the deletion and duplication found in class III aberrant chromosomes could have occurred simultaneously by a nonreciprocal translocation of a telomeric segment of the left arm that replaced a *URA3*-containing segment of the right arm, either within the chromosome or between the homologs. Several sets of inverted repeats across the centromere could contribute to such a translocation (Figure 2). Thus, the right arm junction of each class III subclass contains at least one LTR or Ty1 element in an inverted orientation relative to Ty1-1 and some LTRs on the left arm. PCR was used to determine whether the hypothetical translocation between the inverted repeats actually does occur in the aberrant chromosomes. One primer was set immediately upstream of Ty1-1 and the other was at a centromeric site adjacent to the right arm junction in such a way that both of the primers would point to the right end on the parental chromosome (Figure 4, primers a and c for class III-c). The PCR successfully detected a discrete translocation in all the clones. DNA sequencing of the PCR products revealed that δ 6, δ 7, or Ty1-4 had fused with Ty1-1 to form one complete Ty1 element, which was followed by the region telomeric to Ty1-1 (Figure 4C and Table 1). This was observed in all clones apart from one class III-a clone. If, during the translocation, the Ty1-1-telomeric segment of the left arm replaced the telomeric segment of the right arm, the expected size of the resulting chromosome would agree well with the actual size of the aberrant chromosome detected by PFGE (Table 1). The PCR analysis of the anomalous class III-a clone indicated that it had experienced a translocation that was similar to that observed in another class III-a clone, wherein there was a fusion between δ 6 and Ty1-1. The size of the junction, however, corresponded to two Ty elements instead of one. This clone was not analyzed further due to difficulties in sequencing the region, which might be due to its repeated structure caused by the Ty elements.

In summary, we conclude that all of the class III clones had a nonreciprocal translocation of a telomeric seg-ment of the left arm that replaced a segment of the right arm on chromosome *III*. The translocation utilized an inverted repeat of either Ty1 elements or of Ty1 and δ sequences across the centromere (Table 1). The repeat length is 5.9 kb in the former and ∼330 bp in the latter.

Class III-type translocations are associated with amplification in class IV clones: The ploidy pattern of class IV clones showed some similarities to that of class III, suggesting that the aberrant chromosome *III* of these clones was also generated by a nonreciprocal translocation of the left arm to the right arm of chromosome *III* (Figure 3). In addition, there was an amplification of an internal region on the right arm in class IV clones. In seven clones classified as class IV-a, a region from *III*-153 to *III*-167 had been triplicated. In the remaining clone that was classified as class IV-b, a region from *III*-131 to *III*-167 had been increased to six copies. Southern hybridization probing of the amplified region showed that the aberrant chromosomes gave much stronger signals than their normal homolog and that other chromosomes did not give a signal at all (data not shown). This indicates that the amplification was indeed present on the aberrant chromosome.

The aberrant chromosomes of this class were expected to have a complex construction and thus their overall structure was determined by RFLP analysis using *Mlu*I and *Sac*II (Figure 5). These enzymes do not cut within Ty1 elements. A probe corresponding to the *III*-79 locus was used to detect the region upstream of Ty1-1 while another probe corresponding to the *III*-167 locus was used to locate the amplified region adjacent to Ty1-4. The RFLP analysis revealed three types of chromosome structure in class IV-a clones (Figure 5). In all three, the *III*-79 probe hybridized to two fragments from the aberrant chromosomes. One was the parental fragment from the left arm and the other was a nonparental fragment adjacent to the internal duplication on the right arm. This suggests the involvement of a nonreciprocal translocation of the left arm to the right arm that is similar to those found in class III clones. On the other hand, the internal duplication of the right arm appeared to form a long inverted repeat, judging from the symmetrical positioning of the restriction sites within the region. Thus, at least two types of rearrangements were involved in generating the aberrant chromosome *III* in class IV-a clones, namely, a nonreciprocal translocation of the left arm to the right arm and an inverted duplication within the right arm.

Attempts were made to identify the rearrangement junctions by performing a series of PCR with various primers, followed by DNA sequencing of the products. The junction of the translocation of the left arm was, in fact, contiguous to the inverted duplication within the right arm (Figure 5). At the right end of the inverted duplication, Ty1-2 and/or Ty1-3 sequences were found in an inverted orientation relative to the original ele-
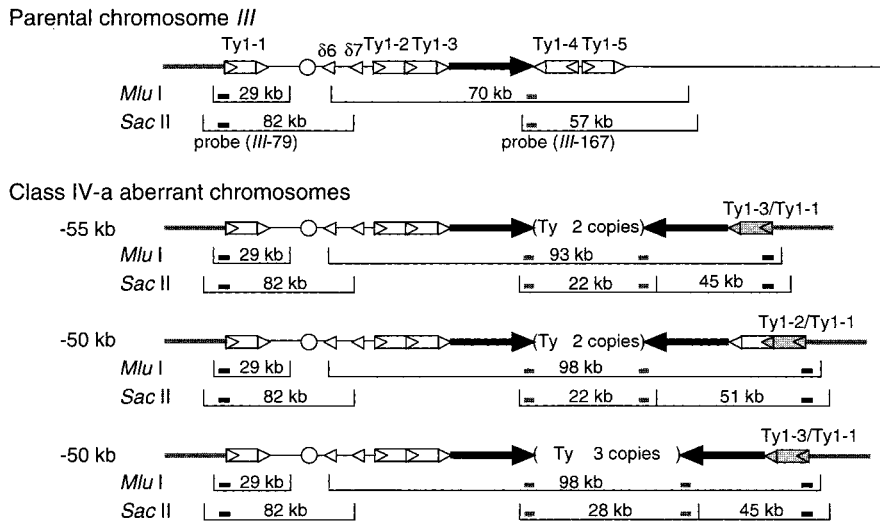
FIGURE 5.—Aberrant chromosomes in class IV-a clones. The structure of three types of aberrant chromosomes in class IV-a are presented schematically and compared with the parental chromosome *III* that contains *MAT*a and the *URA3* insert. Horizontal lines indicate the chromosomes and circles indicate their centromeres. Shaded thick lines indicate the chromosome segment telomeric to Ty1-1 and solid arrows show the segment between Ty1-3 and Ty1-4, respectively, on the parental chromosome. Ty1 elements (rectangles with triangles at the ends) and solo δ sequences (triangles) that were related to the aberrant chromosomes are indicated. The Ty1 element hybrids detected at the breakpoints are shaded. Short bars show the probes used for RFLP analysis at the corresponding positions in the chromosomes. The solid bar indicates the probe corresponding to the *III*-79 locus, while the shaded bar shows the probe corresponding to the *III*-167 locus. The *Mlu*I and *Sac*II restriction fragments detected by the probes are indicated by the segmented lines under each chromosome. The arrangement of the Ty elements in the intervening regions of the inverted duplication (head-to-head solid arrows) was not precisely determined (see text); hence only the copy numbers of Ty elements postulated from the RFLP analysis are indicated in the parentheses. The scale is not proportional.

ments. The Ty1 sequences had been fused with those of Ty1-1, leaving one complete Ty1 element at the joint that was followed by the region telomeric to Ty1-1. The intervening region of the inverted duplication seemed to consist of multiple Ty1 elements that probably contributed to the rearrangement. However, the precise arrangement of the Ty elements could not be determined due to difficulties in amplifying the region, caused presumably by the Ty element repeats in the region.

The aberrant chromosome in the class IV-b clone was analyzed similarly. It contained the same translocation found in the class III-c clones; namely, Ty1-4 on the right arm had been fused with Ty1-1 and this was followed by the region telomeric to Ty1-1 (Table 1). The sixfold multiplied region in this clone was, however, too complicated to be analyzed by RFLP analysis or by a series of PCR with primers specific for various regions on chromosome *III*.

Nonreciprocal translocations between chromosome *III* and other chromosomes in class V clones: In the nine class V clones, a continuous region of chromosome *III* up to its right end was found to be haploid (Figure 3). Class V was further divided into three subclasses according to the junctions of the missing region. The junctions were between *III*-54 and *III*-102 for class V-a, between *III*-141 and *III*-153 for class V-b, and between *III*-167 and *III*-174 for class V-c. Intriguingly, each of these junctions was again within regions that included a cluster of Ty and LTR elements (Figure 2). These observations indicate that class V clones had experienced a gross deletion of chromosome *III* sequences of at least 210 kb for class V-a clones, 160 kb for class V-b clones, and 140 kb for class V-c clones. However, the PFGE analysis of the clones showed that the aberrant

chromosomes were much longer than would be assumed, given these deletions. In fact, some were even longer than the normal chromosome *III* (Table 1). A simple interpretation for this discrepancy would be that the aberrant chromosomes contained an additional portion provided from another chromosome by a translocation. The junction positions identified in the aberrant chromosomes (Figure 3) and the observations made with the other classes suggest that it is highly possible that the translocation in class V clones are also mediated by Ty or LTR elements present on the target chromosome *III* and the other chromosome.

We searched for segments of the appropriate sizes that could be added to form the class V aberrant chromosomes in the SGD database. We focused on only those telomeric segments that have a Ty element at the internal end in the same orientation as the Ty or LTR elements at the junctions on the chromosome *III* side of the aberrant chromosomes. These assumptions were verified with PCR with primers encompassing the presumed translocation junctions, which were designed on the basis of sequences on different chromosomes in the parental strain. The PCR successfully amplified the junctions in six of the nine class V clones. DNA sequencing of the PCR products revealed that the two segments that were originally on different chromosomes were fused at Ty1 elements in such a way as to leave one complete Ty1 element at the joint (Table 1). This structure of class V aberrant chromosomes was confirmed by Southern hybridization of the chromosomes with two probes, one of which hybridized to the chromosome *III* segment and the other of which hybridized to the segment derived from the other chromosome. In all of the six class V clones, the aberrant chromosome was

TABLE 2

Ty1 elements at the breakpoints with complex structures

| Clone name | Class | Ty1 elements at breakpoints | |
		At the original sites (A, B)[a]	Non-A, non-B elements[b]
1	II-a	Ty1-2, Ty1-5	Ty1-3
49	III-b	δ 7, Ty1-1	Ty1-3
9	III-c	Ty1-4, Ty1-1	Ty1-2+Ty1-3
26	IV-a	Ty1-3, Ty1-1	Ty1-1+Ty1-3
2	IV-b	Ty1-4, Ty1-1	Ty1-2
25	V-c	Ty1-4, (*I*) Ty1-1	Ty1-5
35	V-b	Ty1-2, (*VII*) Ty1-1	(*X*) Ty1-2 or (*VII*) Ty1-1+Ty1-2
56	V-b	Ty1-3, (*VII*) Ty1-1	Ty1-2, Ty1-4 or Ty1-5

Ty1 and δ elements are designated with the number that denotes their relative position on the chromosome. The designation of Ty1 elements on chromosome *III* is described in the text, while the designation of the δ element is as given in the SGD database. For the Ty1 elements on chromosomes other than chromosome *III*, the number of the chromosome is indicated in the parentheses in front of the element description.

[a] Ty1 elements detected at the junctions on the parental chromosomes are indicated.

[b] The sequences that are not identical to any of the Ty1 elements at the original sites are referred to as non-A, non-B sequences (see text for details). The Ty1 elements that contain the non-A, non-B sequences are indicated. In the cases of clones 26 and 35, non-A, non-B sequences could be regarded as two discontinuous segments derived from Ty1 elements at the original sites.

visualized with both of the probes (data not shown). For the remaining three clones, we could not identify the junction by these analyses.

Some of the Ty1 elements left at the junction were complex: We determined the entire sequences of the Ty1 elements left at the junctions of 30 recombination events (Tables 1 and 2). In 22 of the 30 examined, the resulting Ty1 element was simple in composition because the two elements at the original sites had become faithfully fused (Table 1 and Figure 6a). That is, the sequence of the Ty1 element at one site (A) was followed by the region identical to both of the two elements (A/B) within which a breakpoint was included and after which the sequence of the Ty1 element from the other site (B) was found. The regions that included the breakpoint (A/B) were dispersed over the entire Ty1 sequence (Figure 6a) and thus no specific resolution site of recombination could be detected. The sequence identity between the Ty1 elements found at the original sites was 96.0–99.6%, while the sequence identity of the δ 6 and Ty1-1 elements found at the breakpoint in a class III-a clone was 90%. The sequence identity of the Ty1 elements in the yeast genome ranges from 60 to nearly 100%. The higher sequence identity observed at the breakpoints is likely to be an important factor that facilitates the homologous recombination between ectopic sites that leads to chromosomal rearrangements.

In eight cases, which were found in clones belonging to Classes II–V, the composition of the conserved Ty1 element was more complex (Table 2 and Figure 6b). This is because of the inclusion of sequences derived from Ty1 elements that were not at the original sites on the parental chromosome. These sequences are denoted as non-A, non-B sequences. The sequences were

bordered on either side by the first nucleotide discontinuous from the original Ty1 element at each end and ranged from 240 to 4526 bp (Figure 6b). Sequences identical to the non-A, non-B regions could be located within other Ty1 elements, mostly in those from chromosome *III* (Table 2). In six cases, non-A, non-B regions could be identified within one Ty1 element as continuous sequences (as a whole, A-C-B), while in the class III-c clone 9, it was divided into two segments that were identified separately within two Ty1 elements (A-C-D-B). Alternatively, in the cases of class IV-a clone 26 and class V-b clone 35, non-A, non-B sequences could be regarded as two discontinuous segments derived from Ty1 elements at the original sites (A-B-A-B). These various constructions could not be explained by simple recombination between the two elements of the original sites.

DISCUSSION

We have systematically analyzed the spontaneous LOH events that lead to functional inactivation of the *URA3* marker that has been hemizygously inserted into chromosome *III* in diploid yeast cells (HIRAOKA *et al.* 2000). About 8% of the clones had acquired an aberrant chromosome derived from chromosome *III*. In the study reported here, we have characterized the breakpoints and the newly formed junctions in the aberrant chromosomes so as to trace the elements involved in the rearrangement process.

Breakpoints of the aberrant chromosomes were within either *MAT-HMR* or Ty1 elements: The identified breakpoints were all within either of two types of repeat sequences, namely, *MAT-HMR* or Ty1 elements (Table 1). The aberration in chromosome *III* in class I clones
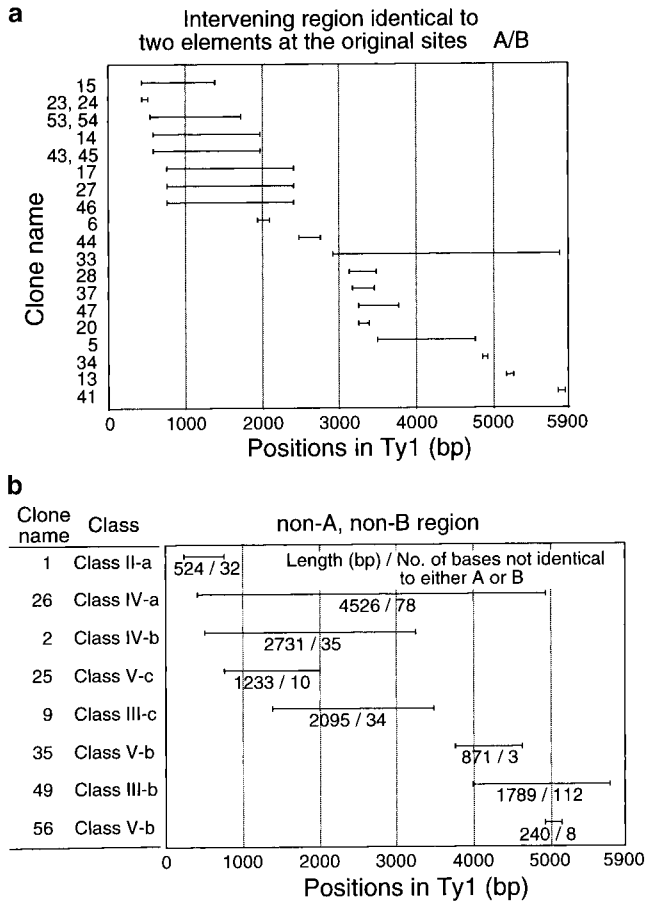
a

Intervening region identical to
two elements at the original sites   A/B

Clone name: 15, 23, 24, 53, 54, 14, 43, 45, 17, 27, 46, 6, 44, 33, 28, 37, 47, 20, 5, 34, 13, 41

Positions in Ty1 (bp): 0 1000 2000 3000 4000 5000 5900

b

Clone name	Class	non-A, non-B region			
1	Class II-a	524 / 32	Length (bp) / No. of bases not identical to either A or B		
26	Class IV-a		4526 / 78		
2	Class IV-b		2731 / 35		
25	Class V-c		1233 / 10		
9	Class III-c		2095 / 34		
35	Class V-b			871 / 3	
49	Class III-b			1789 / 112	
56	Class V-b			240 / 8	

Positions in Ty1 (bp): 0 1000 2000 3000 4000 5000 5900

FIGURE 6.—Composition of the Ty1 elements at the breakpoints. The sequences of the Ty1 elements left at the joints were compared to those in the yeast genome. In 22 of 30 elements, the resulting Ty1 element consisted of two elements at the original sites, designated A and B, respectively. The intervening region identical to both of the original elements (A/B) is shown in a. In the remaining eight cases, the Ty1 element contained continuous sequences that are not found in either of the Ty1 elements at the original sites and are designated non-A, non-B. The non-A, non-B regions are shown in b and are bordered on either side by the first nucleotide discontinuous from the original Ty1 element at each end. The length of the region and the number of bases that are not identical to either of the original Ty1 sequences are indicated.

was a deletion between the direct repeat specific to chromosome *III*, the *MAT*a and *HMR* loci, which are normally 90 kb apart on the right arm. The sequence identity of the 1.6-kb repeat is 99.8%. Our previous studies indicated that this aberration was due to an intrachromosomal deletion in all class I clones (HIRA-OKA *et al.* 2000).

The remaining clones all had an aberrant chromosome *III* due to breakpoints within Ty1 elements located at various sites. In 28 of the 34 class II–V clones, the junction had been formed between 5.9-kb Ty1 elements, while in two other clones it had been formed between Ty1 and the 330-bp δ sequence. Although precise junctions of the remaining four clones could not be deter-

mined, all of the junctions were located within regions that contained these elements (Figure 3). The aberrant chromosomes of class IV-a clones had an additional duplication that also seemed to have been mediated by Ty elements (Figure 5). Ty1 mediation of chromosomal rearrangement occurred regardless of which chromosome was combined with the target chromosome *III*, as Ty1 was involved in the unequal crossing over between the homologous chromosomes (class II clones) as well as in the translocations between other chromosomes (class V clones). In class III and IV clones, nonreciprocal translocations of the left arm to the right arm of chromosome *III* were also mediated by Ty1 elements either between the homologous chromosomes or within the chromosome (probably between the sister chromatids) (Figure 4C).

As the aberrant chromosomes we analyzed had been obtained by the systematic screening of LOH clones, our observations indicate that the majority of the rearrangements of chromosome *III* in diploid cells utilizes two types of homologous sequences, namely, *MAT-HMR* for intrachromosomal deletions and Ty1 elements for various types of translocations. The frequencies of these rearrangements were 3.1×10^{-6} and 6.3×10^{-6}, respectively (HIRAOKA *et al.* 2000), which are 100 times more frequent than nonhomology- or microhomology-mediated rearrangements (CHEN and KOLODNER 1999).

Ty1 elements are likely to play specific roles in chromosomal rearrangements: Ty1 is the most prominent retrotransposon in the yeast genome and 33 copies were found in the haploid genome sequences in the SGD database (HANI and FELDMANN 1998). We identified another five Ty1 elements in the chromosome *III* of the haploid strains that were used to construct the parental diploid RD101. In the yeast genome, there are also other repetitive sequences that are long enough for homologous recombination. Thus, there are 19 full copies of other Ty elements, >250 solo LTRs, and 274 various tRNA genes per haploid genome (HANI and FELDMANN 1998). Although several of the tRNA genes are within the *CEN3-URA3* interval that could be targeted for LOH of the *URA3* marker (Figure 2), these were not, however, found at the breakpoints of the aberrant chromosomes in our analysis. Chromosome *III* is known to have several hot spots for Ty1 integration (JI *et al.* 1993; WARMINGTON *et al.* 1986, 1987; WICKSTEED *et al.* 1994), an observation that is confirmed by this study (Figure 2). This feature may cause Ty1 to play a more prominent role in the alteration of chromosome *III* than might occur in other chromosomes. Nevertheless, our observations furnish definitive evidence that Ty1 elements play specific roles in chromosomal rearrangement.

Ty1 elements appear to mediate various types of rearrangements, occasionally simultaneously, as demonstrated by the class IV clones. In these clones, the aberrant chromosomes had been generated through two different Ty1-mediated rearrangements, namely, a trans-

location and a juxtaposed inverted duplication (Figure 5). In these clones, the inverted duplication had apparently caused the Ty1 elements Ty1-2 and Ty1-3 to become inversely oriented, which then allowed them to act as sites for the translocations that resulted in the LOH. This means that the inverted duplication occurred prior to the translocation. The frequency of these class IV clones bearing the two events was comparable to the frequency of class III clones that had a similar type of translocation. Consequently, class IV clones were unlikely to result from the completely independent double events of duplication and translocation taking place sequentially in the clone. Rather, the translocation and duplication seemed to have occurred simultaneously or through a series of processes that were linked together.

Some of the resulting Ty1 elements left at the breakpoints had complex structures that contained sequences derived from Ty1 elements that were not at the original sites. We have denoted these sequences as non-A, non-B (Table 2 and Figure 6b). Such complex Ty1 elements were found at 23% of Ty1-mediated junctions. Ty1 elements with simple composition (Figure 6a), however, might also contain non-A, non-B segments that could not be recognized from their sequences. It is noteworthy that the non-A, non-B sequences could be identified in other Ty1 elements in the yeast genome, especially in those on chromosome *III* where the rearrangement took place (Table 2). This result suggests that Ty1 elements at more than three different loci frequently participated simultaneously in the rearrangement. The molecular mechanisms underlying these complex rearrangements remain to be resolved. In previous studies, such complex Ty1 elements were also observed in the joint left by the intrachromosomal deletion between Ty1 elements, as detected by RFLP analyses (ROEDER and FINK 1982; ROEDER *et al.* 1984). Roeder and Fink suggested that gene conversion involving Ty1 elements at three different sites could generate a new Ty1 sequence at the site of rearrangement (ROEDER and FINK 1982). Alternatively, cDNA of Ty1 elements might donate the non-A, non-B sequences. MELAMED *et al.* (1992) suggested that Ty1 cDNA might be involved in some types of homologous recombination between Ty1 elements. It has also been reported that a piece of a Ty1 element can be inserted at a site of double-strand break (DSB) during its nonhomologous repair (MOORE and HABER 1996) and that reverse transcriptases of retroelements were necessary for the process (TENG *et al.* 1996). All of these observations suggest that Ty1 elements play more important roles in chromosomal rearrangement than just providing homologous sequences.

These observations also explain why clones with an aberrant chromosome *V* could not be identified when we performed a similar analysis on LOH of the autologous *URA3* locus present on the left arm of chromosome *V* (HIRAOKA *et al.* 2000). According to the SGD database, Ty1 and other Ty elements are not present within the 35-kb interval between *CEN5* and *URA3* on chromosome *V*. This may also be the reason behind the limited chromosome *V* rearrangements in haploid cells that were assessed for the simultaneous loss of two separated markers on the left arm of chromosome *V* (CHEN and KOLODNER 1999). However, it is also possible that many, perhaps grosser, rearrangements that occur in haploid cells might go unrecognized because they result in the loss of an essential gene or DNA segment that makes the cell inviable.

Possible pathways of homologous recombination that lead to aberrant chromosomes: In our previous analysis of the spontaneous LOH events for the *URA3* marker that had been hemizygously inserted at *III*-205, the genetic alterations leading to LOH occurred at a frequency of $1–2 \times 10^{-4}$ (HIRAOKA *et al.* 2000). The genetic changes were largely the result of allelic recombination and chromosome loss. Allelic recombination contributed to 30–35% of all the LOH events, while chromosome loss was responsible for ∼60%. For the latter monosomic clones, the remaining normal-sized chromosome was shown in 4% of the clones to be the recombinant chromosome between the homologous chromosomes *III*. It was concluded that a certain portion of recombination events occurs in a nonconservative fashion and thus contributes to chromosome loss (HIRAOKA *et al.* 2000). It is possible that the class II-b and II-c clones, which have only one chromosome (which is also aberrant), have lost their other chromosome *III* via a similar mechanism. These clones were shown to have an aberrant chromosome *III* that had been formed by unequal crossing over between the homologs (Table 1). Thus, the recombination process had presumably occurred in a nonconservative way and this resulted in the loss of the other homolog. The remaining 8% of the LOH clones had acquired the aberrant chromosomes that are the subject of this study. As shown in Table 1, ectopic recombination that generated the aberrant chromosomes had occurred exclusively between repetitive sequences such as *MAT-HMR*, Ty1, and δ sequences. In either case, the repeats seem to be long enough to mediate homologous recombination in yeast cells. While recombination mediated by Ty1 elements has special features, as discussed above, our observations indicate that homologous recombination contributes to at least half of the chromosome alterations that lead to LOH and that this can manifest itself in multiple ways, including the generation of aberrant chromosomes, allelic recombination, and a certain kind of chromosome loss.

The aberrant chromosomes analyzed in this study could be generated by several mechanisms of homologous recombination (PAQUES and HABER 1999). The aberrant chromosomes in the class II–V clones could have been the result of unequal crossing over or translocation that occurred between a Ty1 element in the genome and a Ty1 element within the *URA3-CEN3* interval on the target chromosome *III*. Such reciprocal recombination could give rise to LOH cells if the recombi-

nation reaction occurred between nonsister chromatids during S or G2 phase. For the class III and IV clones, the translocations of the left arm to the right arm of chromosome *III* could also occur between the sister chromatids, which end with the same consequence as the translocations between the homologous chromatids. That these recombination events occur in the S phase is a particularly attractive idea because the replication process produces many single-strand nicks or gaps that may serve as initiation sites for the recombination reactions. Alternatively, break-induced replication initiated at a Ty1 element could be the mechanism that induces the nonreciprocal replacement of the telomeric segment that includes the *URA3* marker on the target chromosome *III* with a telomeric segment from another chromosome (MALKOVA *et al.* 1996; MORROW *et al.* 1997). Such DSBs within the interval of *URA3* and *CEN3* could be formed endogenously in normally growing cells during the various processes of DNA metabolism. Since all of the aberrant chromosomes we analyzed carried a deletion in the target chromosome (Figure 3), it is also possible that single-strand annealing after a DSB generates an aberrant chromosome *III* (LIN *et al.* 1984; MARYON and CARROLL 1991; SUGAWARA and HABER 1992). That is, a DSB between *URA3* and *CEN3* could be repaired with another DSB through the annealing of Ty1 sequences. In either case, the resulting chromosome could differ in size depending on the positions of Ty1 elements involved in the reaction. The intrachromosomal deletion between the *MAT* and *HMR* loci in the class I clones may also be caused by single-strand annealing that repairs a spontaneous DSB generated between the loci. Another mechanism possible for the deletion could be through unequal crossing over or break-induced replication between sister chromatids of the target chromosome *III*. It is not clear why the *MAT-HMR* repeat was not utilized by unequal crossing over between the homologous chromosomes *III*. Incidentally, although there exist >10 direct repeats of solo LTRs and of LTRs and Ty elements across the *URA3* insert on the right arm of chromosome *III*, intrachromosomal deletions between the repeats did not occur at a detectable level in our screening (HIRAOKA *et al.* 2000). To identify the mechanism responsible for each event, we are now examining the effects of several recombination-deficient mutations on the LOH events.

LITERATURE CITED

AUSUBEL, F. M., R. BRENT, R. E. KINGSTON, D. D. MOORE, J. G. SEIDMAN *et al.*, 1994 *Current Protocols in Molecular Biology*. John Wiley & Sons, New York.

BREILMANN, D., J. GAFNER and M. CIRIACY, 1985 Gene conversion and reciprocal exchange in a *Ty*-mediated translocation in yeast. Curr. Genet. **9:** 553–560.

CHEN, C., and R. D. KOLODNER, 1999 Gross chromosomal rearrangements in *Saccharomyces cerevisiae* replication and recombination defective mutants. Nat. Genet. **23:** 81–85.

CHEN, C., K. UMEZU and R. D. KOLODNER, 1998 Chromosomal rearrangements occur in *S. cerevisiae rfa1* mutator mutants due to mutagenic lesions processed by double-strand-break repair. Mol. Cell **2:** 9–22.

CHRISTMAN, M. F., F. S. DIETRICH and G. R. FINK, 1988 Mitotic recombination in the rDNA of *S. cerevisiae* is suppressed by the combined action of DNA topoisomerases I and II. Cell **55:** 413–425.

DOWNS, K. M., G. BRENNAN and S. W. LIEBMAN, 1985 Deletions extending from a single *Ty1* element in *Saccharomyces cerevisiae*. Mol. Cell. Biol. **5:** 3451–3457.

GUPTA, P. K., A. SAHOTA, S. A. BOYADJIEV, S. BYE, C. SHAO *et al.*, 1997 High frequency *in vivo* loss of heterozygosity is primarily a consequence of mitotic recombination. Cancer Res. **57:** 1188–1193.

HANI, J., and H. FELDMANN, 1998 tRNA genes and retroelements in the yeast genome. Nucleic Acids Res. **26:** 689–696.

HIRAOKA, M., K. WATANABE, K. UMEZU and H. MAKI, 2000 Spontaneous loss of heterozygosity in diploid *Saccharomyces cerevisiae* cells. Genetics **156:** 1531–1548.

JI, H., D. P. MOORE, M. A. BLOMBERG, L. T. BRAITERMAN, D. F. VOYTAS *et al.*, 1993 Hotspots for unselected *Ty1* transposition events on yeast chromosome *III* are near tRNA genes and *LTR* sequences. Cell **73:** 1007–1018.

KEIL, R. L., and A. D. MCWILLIAMS, 1993 A gene with specific and global effects on recombination of sequences from tandemly repeated genes in *Saccharomyces cerevisiae*. Genetics **135:** 711–718.

KLEIN, H. L., 1995 Genetic control of intrachromosomal recombination. Bioessays **17:** 147–159.

KNUDSON, A. G., 1993 Antioncogenes and human cancer. Proc. Natl. Acad. Sci. USA **90:** 10914–10921.

KUPIEC, M., and T. D. PETES, 1988 Allelic and ectopic recombination between *Ty* elements in yeast. Genetics **119:** 549–559.

LASKO, D., W. CAVENEE and M. NORDENSKJOLD, 1991 Loss of constitutional heterozygosity in human cancer. Annu. Rev. Genet. **25:** 281–314.

LIEBMAN, S., P. SHALIT and S. PICOLOGLOU, 1981 *Ty* elements are involved in the formation of deletions in *DEL1* strains of *Saccharomyces cerevisiae*. Cell **26:** 401–409.

LIN, F. L., K. SPERLE and N. STERNBERG, 1984 Model for homologous recombination during transfer of DNA into mouse L cells: role for DNA ends in the recombination process. Mol. Cell. Biol. **4:** 1020–1034.

MALKOVA, A., E. L. IVANOV and J. E. HABER, 1996 Double-strand break repair in the absence of *RAD51* in yeast: a possible role for break-induced DNA replication. Proc. Natl. Acad. Sci. USA **93:** 7131–7136.

MARYON, E., and D. CARROLL, 1991 Characterization of recombination intermediates from DNA injected into *Xenopus laevis* oocytes: evidence for a nonconservative mechanism of homologous recombination. Mol. Cell. Biol. **11:** 3278–3287.

MELAMED, C., Y. NEVO and M. KUPIEC, 1992 Involvement of cDNA in homologous recombination between *Ty* elements in *Saccharomyces cerevisiae*. Mol. Cell. Biol. **12:** 1613–1620.

MOORE, J. K., and J. E. HABER, 1996 Capture of retrotransposon DNA at the sites of chromosomal double-strand breaks. Nature **383:** 644–646.

MORROW, D. M., C. CONNELLY and P. HIETER, 1997 "Break copy" duplication: a model for chromosome fragment formation in *Saccharomyces cerevisiae*. Genetics **147:** 371–382.

MYUNG, K., A. DATTA, C. CHEN and R. D. KOLODNER, 2001a SGS1, the Saccharomyces cerevisiae homologue of BLM and WRN, suppresses genome instability and homeologous recombination. Nat. Genet. **27:** 113–116.

MYUNG, K., A. DATTA and R. D. KOLODNER, 2001b Suppression of spontaneous chromosomal rearrangements by S phase checkpoint functions in Saccharomyces cerevisiae. Cell **104:** 397–408.

OLIVER, S. G., Q. J. VAN DER AART, M. L. AGOSTONI-CARBONE, M. AIGLE, L. ALBERGHINA *et al.*, 1992 The complete DNA sequence of yeast chromosome *III*. Nature **357:** 38–46.

PAQUES, F., and J. E. HABER, 1999   Multiple pathways of recombination induced by double-strand breaks in Saccharomyces cerevisiae. Microbiol. Mol. Biol. Rev. **63:** 349–404.

RACHIDI, N., P. BARRE and B. BLONDIN, 1999   Multiple *Ty*-mediated chromosomal translocations lead to karyotype changes in a wine strain of *Saccharomyces cerevisiae*. Mol. Gen. Genet. **261:** 841–850.

ROEDER, G. S., and G. R. FINK, 1980   DNA rearrangements associated with a transposable element in yeast. Cell **21:** 239–249.

ROEDER, G. S., and G. R. FINK, 1982   Movement of yeast transposable elements by gene conversion. Proc. Natl. Acad. Sci. USA **79:** 5621–5625.

ROEDER, G. S., M. SMITH and E. J. LAMBIE, 1984   Intrachromosomal movement of genetically marked *Saccharomyces cerevisiae* transposons by gene conversion. Mol. Cell. Biol. **4:** 703–711.

ROSE, M. D., F. WINSTON and P. HIETER, 1990   *Methods in Yeast Genetics: A Laboratory Course Manual*. Cold Spring Harbor Laboratory Press, Cold Spring Harbor, NY.

ROTHSTEIN, R., 1979   Deletions of a tyrosine tRNA gene in *S. cerevisiae*. Cell **17:** 185–190.

ROTHSTEIN, R., C. HELMS and N. ROSENBERG, 1987   Concerted deletions and inversions are caused by mitotic recombination between delta sequences in *Saccharomyces cerevisiae*. Mol. Cell. Biol. **7:** 1198–1207.

SAMBROOK, J., E. F. FRITSCH and T. MANIATIS, 1989   *Molecular Cloning: A Laboratory Manual*. Ed. 2. Cold Spring Harbor Laboratory Press, Cold Spring Harbor, NY.

SUGAWARA, N., and J. E. HABER, 1992   Characterization of double-strand break-induced recombination: homology requirements and single-stranded DNA formation. Mol. Cell. Biol. **12:** 563–575.

TENG, S. C., B. KIM and A. GABRIEL, 1996   Retrotransposon reverse-transcriptase-mediated repair of chromosomal breaks. Nature **383:** 641–644.

TISCHFIELD, J. A., 1997   Loss of heterozygosity or: how I learned to stop worrying and love mitotic recombination. Am. J. Hum. Genet. **61:** 995–999.

WARMINGTON, J. R., R. ANWAR, C. S. NEWLON, R. B. WARING, R. W. DAVIES *et al.*, 1986   A 'hot-spot' for *Ty* transposition on the left arm of yeast chromosome *III*. Nucleic Acids Res. **14:** 3475–3485.

WARMINGTON, J. R., R. P. GREEN, C. S. NEWLON and S. G. OLIVER, 1987   Polymorphisms on the right arm of yeast chromosome *III* associated with *Ty* transposition and recombination events. Nucleic Acids Res. **15:** 8963–8982.

WICKSTEED, B. L., I. COLLINS, A. DERSHOWITZ, L. I. STATEVA, R. P. GREEN *et al.*, 1994   A physical comparison of chromosome *III* in six strains of *Saccharomyces cerevisiae*. Yeast **10:** 39–57.